

## Sensitivity analyses of OH missing sinks over Tokyo metropolitan area in the summer of 2007

S. Chatani<sup>1,\*</sup>, N. Shimo<sup>1</sup>, S. Matsunaga<sup>1</sup>, Y. Kajii<sup>2</sup>, S. Kato<sup>2</sup>, Y. Nakashima<sup>2</sup>, K. Miyazaki<sup>2</sup>, K. Ishii<sup>3</sup>, and H. Ueno<sup>3</sup>

<sup>1</sup>Japan Petroleum Energy Center, Tokyo, Japan

<sup>2</sup>Tokyo Metropolitan University, Tokyo, Japan

<sup>3</sup>Tokyo Metropolitan Research Institute for Environmental Protection, Tokyo, Japan

\*Contracted researcher from Toyota Central R&D Labs., Inc., Aichi, Japan

Received: 8 July 2009 – Published in Atmos. Chem. Phys. Discuss.: 4 September 2009

Revised: 19 November 2009 – Accepted: 19 November 2009 – Published: 27 November 2009

**Abstract.** OH reactivity is one of key indicators which reflect impacts of photochemical reactions in the atmosphere. An observation campaign has been conducted in the summer of 2007 at the heart of Tokyo metropolitan area to measure OH reactivity. The total OH reactivity measured directly by the laser-induced pump and probe technique was higher than the sum of the OH reactivity calculated from concentrations and reaction rate coefficients of individual species measured in this campaign. And then, three-dimensional air quality simulation has been conducted to evaluate the simulation performance on the total OH reactivity including “missing sinks”, which correspond to the difference between the measured and calculated total OH reactivity. The simulated OH reactivity is significantly underestimated because the OH reactivity of volatile organic compounds (VOCs) and missing sinks are underestimated. When scaling factors are applied to input emissions and boundary concentrations, a good agreement is observed between the simulated and measured concentrations of VOCs. However, the simulated OH reactivity of missing sinks is still underestimated. Therefore, impacts of unidentified missing sinks are investigated through sensitivity analyses. In the cases that unknown secondary products are assumed to account for unidentified missing sinks, they tend to suppress formation of secondary aerosol components and enhance formation of ozone. In the cases that unidentified primary emitted species are assumed to account for unidentified missing sinks, a variety of impacts may be

observed, which could serve as precursors of secondary organic aerosols (SOA) and significantly increase SOA formation. Missing sinks are considered to play an important role in the atmosphere over Tokyo metropolitan area.

### 1 Introduction

Air quality in Japan has been improved, however, some problems are still remained unresolved. NO<sub>2</sub> concentrations at some roadside monitoring stations located in urban area exceed the Environmental Quality Standards (EQSs) in Japan. O<sub>3</sub> concentrations are gradually increasing and the EQSs for photochemical oxidants have not been satisfied at almost all monitoring stations in whole Japan (Ministry of the Environment, 2008). In addition, PM<sub>2.5</sub> concentrations in Japanese urban areas are likely higher than the air quality standards implemented in the US and Europe.

Most of NO<sub>2</sub>, O<sub>3</sub> and PM<sub>2.5</sub> are secondarily produced through photochemical reactions in the atmosphere. Their concentrations nonlinearly respond to emissions of various precursors (Meng et al., 1997). In order to consider how to reduce concentrations of secondary products, it is necessary to perform simulations using a three-dimensional air quality model in which complex photochemical reactions are involved. However, it is inevitably important to determine the reliability of the simulation results, that is, whether simulated responses of secondary products to precursor emissions are reliable. Observation data of critical pollutants (e.g. NO<sub>2</sub> and O<sub>3</sub>) are mainly used for validation, but more thorough validation is desirable.



Correspondence to: S. Chatani  
(schatani@mosk.tytlabs.co.jp)

Though progresses in measuring instruments and techniques have realized identification of various trace species, many atmospheric trace species have remained unidentified. Their importance on photochemical reactions needs to be evaluated. Total OH reactivity is one of key indicators which reflect the impacts of identified and unidentified species on photochemical reactions and secondary products. It is also useful as an indicator to validate the three-dimensional air quality simulations in terms of complex photochemical reactions.

A technique to directly measure total OH reactivity has been developed by Sadanaga et al. (2004b, 2005b) and Yoshino et al. (2006) used this technique to perform direct measurement of total OH reactivity at Hachioji, Japan, which is located about 30 km west of the heart of Tokyo metropolitan area. As well as total OH reactivity, they measured concentrations of various species and calculated OH reactivity from concentrations of measured species and their known reaction rate coefficients with OH. They found that the directly measured total OH reactivity was always higher than the sum of the OH reactivity of measured individual species. The difference between the measured and calculated total OH reactivity is called “missing sinks”, which may affect photochemical reactions and secondary product formation in the atmosphere.

In order to further investigate the impacts of missing sinks within the metropolitan area, an observation campaign has been conducted in the summer of 2007 at the heart of Tokyo metropolitan area. Total OH reactivity and concentrations of various species were measured in this campaign. And then, we executed the three-dimensional air quality model and compared the simulation results with the observation results. The air quality models treat photochemical reactions in aggregated forms as in CB4 (Gery et al., 1989) and SAPRC99 (Carter, 2000) chemical mechanisms. Missing sinks should be part of some aggregated species groups defined in the chemical mechanisms. To validate the simulations in terms of photochemical reactions, we have examined whether the simulation can reproduce the measured total OH reactivity including missing sinks. In addition, we have conducted sensitivity analyses to investigate the impacts of missing sinks on photochemical reactions and secondary products.

Measurements of total OH reactivity were conducted also in other countries. Di Carlo et al. (2004) measured total OH reactivity in a northern Michigan forest. The airborne measurements of total OH reactivity were conducted by Mao et al. (2009) during INTEX-B observation campaign which was focused on the Asian pollution outflow over Pacific Ocean. In the urban environment, total OH reactivity was measured at New York City (Ren et al., 2003), Mexico City (Shirley et al., 2006), Mainz (Sinha et al., 2008), and Guangzhou (Hofzumahaus et al., 2009). Most of these studies have implied existence of missing sinks in the atmosphere. Simple steady-state calculations and box model simulations in which detailed chemical mechanisms are incorporated are often

used to analyse measurement results, but comparison with three-dimensional air quality simulations has been scarce.

On the other hand, validations of three-dimensional air quality simulations have been conducted recently in terms of OH reactivity. Steiner et al. (2008) and Stroud et al. (2008) investigated OH reactivity in central California and Canada, respectively. They calculated OH reactivity from measured and simulated concentrations of various species, and compared them. However, measured total OH reactivity and missing sinks were not used directly in these papers. In this study, simulated OH reactivity is compared with the directly measured OH reactivity including missing sinks. In addition, impacts of missing sinks are investigated through sensitivity analyses.

An overview of the three-dimensional air quality simulations are described in Sect. 2. A brief description of the observation campaign is provided in Sect. 3. Performance of the three-dimensional air quality simulation for OH reactivity is described in Sect. 4. Results of sensitivity analyses of missing sinks are described in Sect. 5. And the outcomes are summarized in Sect. 6.

## 2 Overview of three-dimensional air quality simulations

We have developed a three-dimensional air quality simulation framework which consists of the Weather Research and Forecasting (WRF) model for meteorology, the Community Multi-scale Air Quality (CMAQ) modeling system for pollutant concentrations, and emission inventory models. Details of the simulation are described below.

### 2.1 Target domains

Target domains of the three-dimensional air quality simulations are shown in Fig. 1. Three nested domains are used in the simulation: East Asia, Japan, and Kanto (including Tokyo metropolitan area). Horizontal coordinate system is based on Lambert conformal conic projection and the reference latitude and longitude coordinates are given as 36 N, 128 E for East Asia domain, and 38.1 N, 136.9 E for Japan and Kanto domains. Domain dimensions for WRF are 5832×4248 km for East Asia, 2000×2000 km for Japan and 336×384 km for Kanto region, respectively, while for CMAQ, slightly smaller domains are given. Vertical coordinate system is based on the sigma-P coordinate system and the top pressure is 100 hPa. The number of vertical layers of East Asia, Japan and Kanto domains for WRF is 31, 34 and 34, respectively, while for CMAQ, the number is merged into 20, 23 and 23, respectively. Approximate height of bottom layer is 57 m in East Asia, and 16 m in Japan and Kanto domains. Grid dimensions are 36×36 km for East Asia, 16×16 km for Japan and 4×4 km for Kanto domain, respectively. In WRF simulation, calculations of East Asia

domain are done separately, while calculations of Japan and Kanto domains are done simultaneously using a two-way nesting approach. In CMAQ simulation, calculations of East Asia, Japan and Kanto domains are done consecutively using a one-way nesting approach.

## 2.2 Input emission data

Motor vehicle emission inventory model developed under Japan AuTo-Oil Program (JATOP) (Japan Petroleum Energy Center, 2009) is used to calculate motor vehicle emission inventories in Japan. The model can estimate hourly running, start and evaporative emissions. Georeference-Based Emission Activity Modeling System (GBEAMS) (Nansai et al., 2004) is used to calculate hourly emissions from anthropogenic sources except for vehicles in Japan. Regional Emission inventory in ASia (REAS) ver. 1.11 (Ohara et al., 2007) is used for preparing anthropogenic emissions in East Asia domain. Model of Emissions of Gases and Aerosols from Nature (MEGAN) v2.04 (Guenther et al., 2006) is used to estimate biogenic VOC emissions.

## 2.3 Meteorology and air quality models

WRF-ARW ver. 2.2.1 (Skamarock et al., 2005) is used to prepare meteorological fields. NCEP Final Analysis data are used to provide initial and boundary conditions, and to perform grid nudging. CMAQ ver. 4.6 (Byun et al., 2006) is used to simulate pollutant concentrations in the atmosphere. The default datasets provided with CMAQ are used as initial concentrations in all domains and boundary concentrations in East Asia domain. Simulations are started one month before the observation campaign as a spin-up period to eliminate influence of initial concentrations. SAPRC99 (Carter, 2000) is chosen for the chemical mechanism. Table 1 shows relationships between the species measured in the observation campaign and the SAPRC99 species which react with OH. Measured species are allocated to one of the SAPRC99 species. These SAPRC99 species are further merged into species groups - abbreviated as AVOC, BVOC and OVOC - as shown in Table 1. However, no measured species are allocated to the SAPRC99 species listed in the "missing sinks" group in Table 1, which are treated as missing sinks in this paper.

## 3 Overview of the observation campaign

Overview of the observation campaign is described in this section. And the details have been published by Nakashima et al. (2009).

An observation campaign has been conducted from 21 to 29 August 2007 in Koto-Ku, Tokyo, which is close to the heart of Tokyo metropolitan area as shown in Fig. 1. OH reactivity and VOC concentrations were measured during daytime of 21, 22, 23, 26 and 27 August. Wind direction was

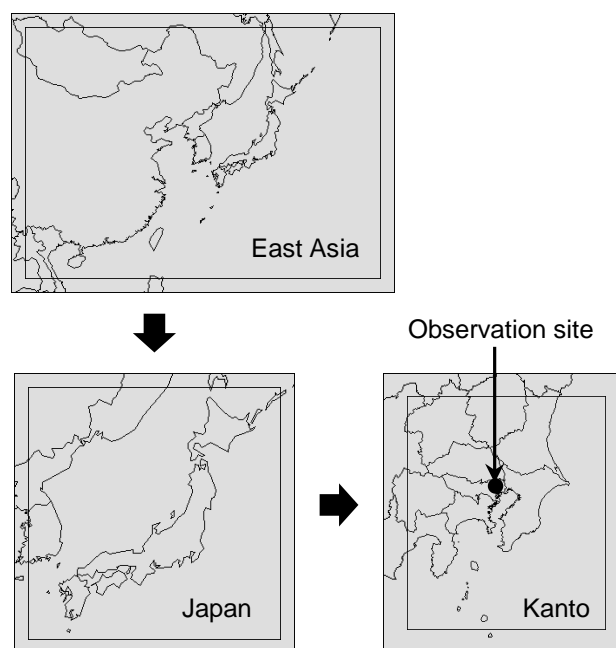


**Fig. 1.** Target domains of the simulation, with outer lines indicating WRF domains, while inner lines indicating CMAQ domains, and showing the position of the observation site.

consistently southerly but changed to north-westerly only on 23 August. In order to avoid influences of different wind directions, data obtained on 21, 22, 26 and 27 August are used for the analysis of this paper. Ambient air is introduced into the reaction flow tube. A laser beam is used to irradiate the incident window of the reaction tube and OH radicals are artificially generated. Changes in OH concentrations are detected by the laser-induced pump and probe technique. Total OH reactivity is represented by the decay rate of OH. In addition, measurements have been conducted on concentrations of critical species ( $\text{NO}_2$ ,  $\text{NO}$ ,  $\text{O}_3$ ,  $\text{CO}$  and  $\text{SO}_2$ ), various individual non-methane hydrocarbons (NMHCs) and oxygenated volatile organic compounds (OVOCs). All of measured species and corresponding SAPRC99 species are listed in Table 1. It must be stated that some of species listed in Table 1 react with not only OH but also  $\text{NO}_3$ ,  $\text{O}_3$  and other species in the real atmosphere and simulations. However, they exclusively react with OH in the reaction tube because concentration of generated OH is much higher than other reactants. Therefore, interference by reactions with other reactants can be ignored.

Figure 2 shows the directly measured and calculated total OH reactivity, of which calculations are obtained from concentrations and reaction rate coefficients of the measured species on 21 August, as an example. Existing databases (Atkinson, 2004, 2007; Atkinson et al., 1997; Calvert et al., 2000; Sander et al., 2002) are used for reaction rate coefficients except for the rate coefficient for the  $\text{NO}_2 + \text{OH}$

**Table 1.** Relationships among species group, SAPRC99 species and individual species measured in the observation campaign in this study.

Species group	SAPRC99 species	Measured species
NO <sub>2</sub>	NO2	NO <sub>2</sub>
NO	NO	NO
O <sub>3</sub>	O3	O <sub>3</sub>
CO	CO	CO
SO <sub>2</sub>	SO2	SO <sub>2</sub>
AVOC	ALK1	ethane
	ALK2	acetylene, propane
	ALK3	isobutane, n-butane, 2,2-dimethylbutane
	ALK4	2,3-dimethylbutane, isopentane, n-pentane, cyclopentane, 2-methylpentane, 3-methylpentane, n-hexane, methylcyclopentane, 2,4-dimethylpentane, 2,2,4-trimethylpentane
	ALK5	cyclohexane, 2-methylhexane, 2,3-dimethylpentane, 3-methylhexane, n-heptane, methylcyclohexane, 2,3,4-trimethylpentane, 2-methylheptane, 3-methylheptane, n-octane, n-nonane
	ETHENE	Ethene
	OLE1	propylene, 1-butene, 3-methyl-1-butene, 1-pentene, 4-methyl-1-pentene
	OLE2	butadiene, trans-2-butene, cis-2-butene, trans-2-pentene, cis-2-pentene, 2-methyl-2-butene, cyclopentene, 2-methyl-1-pentene, trans-2-hexene, cis-2-hexene, styrene
	ARO1	benzene, toluene, ethylbenzene, iso-propylbenzene, n-propylbenzene
	ARO2	p,m-xylene, o-xylene, 1,3,5-trimethylbenzene, 1,2,4-trimethylbenzene
BVOC	ISOPRENE	Isoprene
	TRP1	$\alpha$ -pinene, camphene, $\beta$ -pinene, limonene
OVOC	MEOH	methanol
	HCHO	formaldehyde
	CCHO	acetaldehyde
	ACET	acetone
Missing sinks	NO <sub>3</sub> , HNO <sub>3</sub> , HONO, HO <sub>2</sub> , HNO <sub>4</sub> , HO <sub>2</sub> H, COOH, ROOH, RNO <sub>3</sub> , MEK, PROD <sub>2</sub> , CCO_OOH, RCO.OH, PHEN, HCOOH, RCHO, GLY, MGLY, CRES, BALD, METHACRO, MVK, ISOPROD, DCB1, DCB2, DCB3	

reaction. The rate coefficient for the NO<sub>2</sub>+OH reaction has large uncertainty. Sadanaga et al. (2004a) mentioned discrepancy in it among major databases and its importance for evaluation of OH reactivity. Then, Sadanaga et al. (2005a) measured the rate coefficient for the NO<sub>2</sub>+OH reaction under the atmospheric pressure. This value is used in this study. The directly measured values of total OH reactivity are mostly higher than the sum of the calculated OH reactivity. It implies the existence of missing sinks in the atmosphere over Tokyo metropolitan area.

Figure 3 shows contribution of species groups to the directly measured OH reactivity which is averaged over the target period. NO<sub>2</sub> and AVOC are major contributors, but fraction of the missing sinks is larger than that of NO<sub>2</sub> and AVOC. Therefore, it implies that missing sinks are playing

an important role in photochemical reactions and secondary product formation in the atmosphere over Tokyo metropolitan area.

It must be noted that measurements of OH reactivity and concentrations of chemical species as well as published rate constants contain uncertainties. However, Yoshino et al. (2006) concluded that missing sinks which were derived from the same instrumental setup cannot be explained by uncertainties. They showed clear seasonal dependence in which missing sinks became negligible in winter. It implies that missing sinks are related to photochemical activities, not to systematic uncertainties. In addition, influences of missing sinks must be evaluated even if some uncertainties are contained. They can be recognized as one of uncertainties in simulation results caused by uncertainties in measurements

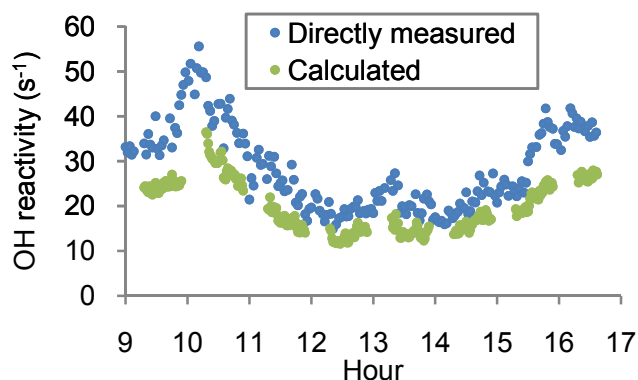


**Fig. 2.** Directly measured and calculated total OH reactivity, of which calculations are obtained from concentrations and reaction rate coefficients of the measured species on 21 August.

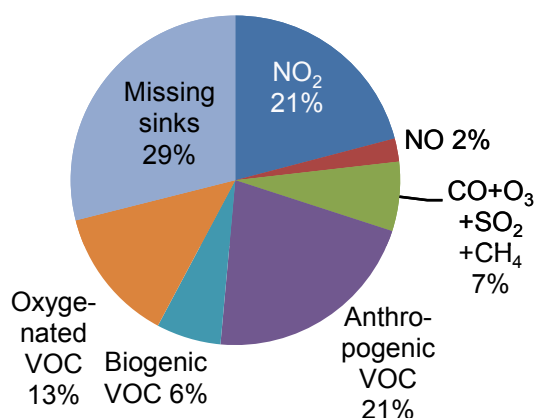


**Fig. 3.** Contribution of species groups to directly measured OH reactivity which is averaged over the target period.

as well as missing sinks which really exist in the atmosphere. They are within the scope of this study.

#### 4 Results of the simulation

The three-dimensional air quality simulation was executed for the period including daytime of 21, 22, 26 and 27 August 2007. Figure 4 shows ratios of the simulated concentrations to the measured concentrations of SAPRC99 species which is averaged over the target period. Ratios of almost all of SAPRC99 VOC species are significantly lower than 1.0. The most probable reason for the underestimation is due to the emission inventory. Solvent use is recognized as a major contributing source to total VOC emissions in Japan (Kanari et al., 2007), however, the emission estimates have large uncertainty. Their special and temporal distribution is also not well known. Obviously, more works are required to improve the emission inventory estimation, especially for VOC emissions. Another possible reason for the underestimation

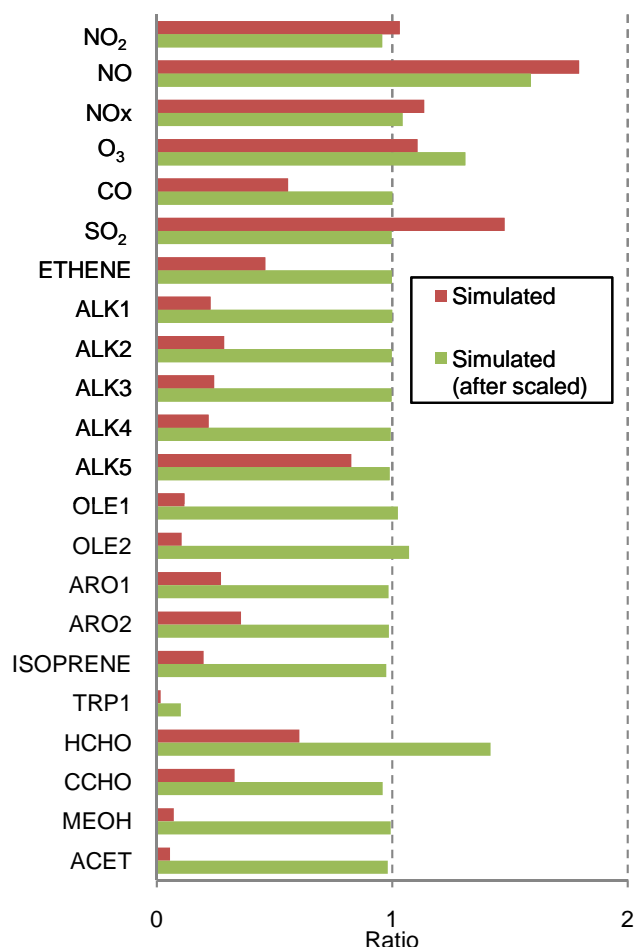


**Fig. 4.** Ratios of simulated to measured concentrations of SAPRC99 species which are averaged over the target period before and after application of scaling factors.

is meteorological conditions during the observation campaign. Wind direction in daytime is mostly southerly during the target period. The observation site is located in a few kilometres north of Tokyo Bay. There are few major pollutant sources in the south of the measurement site. It is well known that pollutant distribution over the coastal area of Tokyo Bay is affected by sea-land breeze and heat-island effect (Yoshikado, 1992). It is considered the simulation may have difficulty in reproducing detailed wind flow patterns caused by these factors.

Here, we assume a situation where the challenges in simulation stated above are resolved. Scaling factors for each SAPRC99 species are uniformly applied to input emissions and boundary concentrations. Scaling factors are defined by inverse numbers of the ratios shown in Fig. 4. The same scaling factors determined from  $\text{NO}_x$  ( $\text{NO} + \text{NO}_2$ ) are applied to  $\text{NO}$  and  $\text{NO}_2$  to keep the ratios of  $\text{NO}$  and  $\text{NO}_2$  in  $\text{NO}_x$  emissions.  $\text{O}_3$  has no emission and scaling factors are applied only to boundary concentration. This procedure is repeated

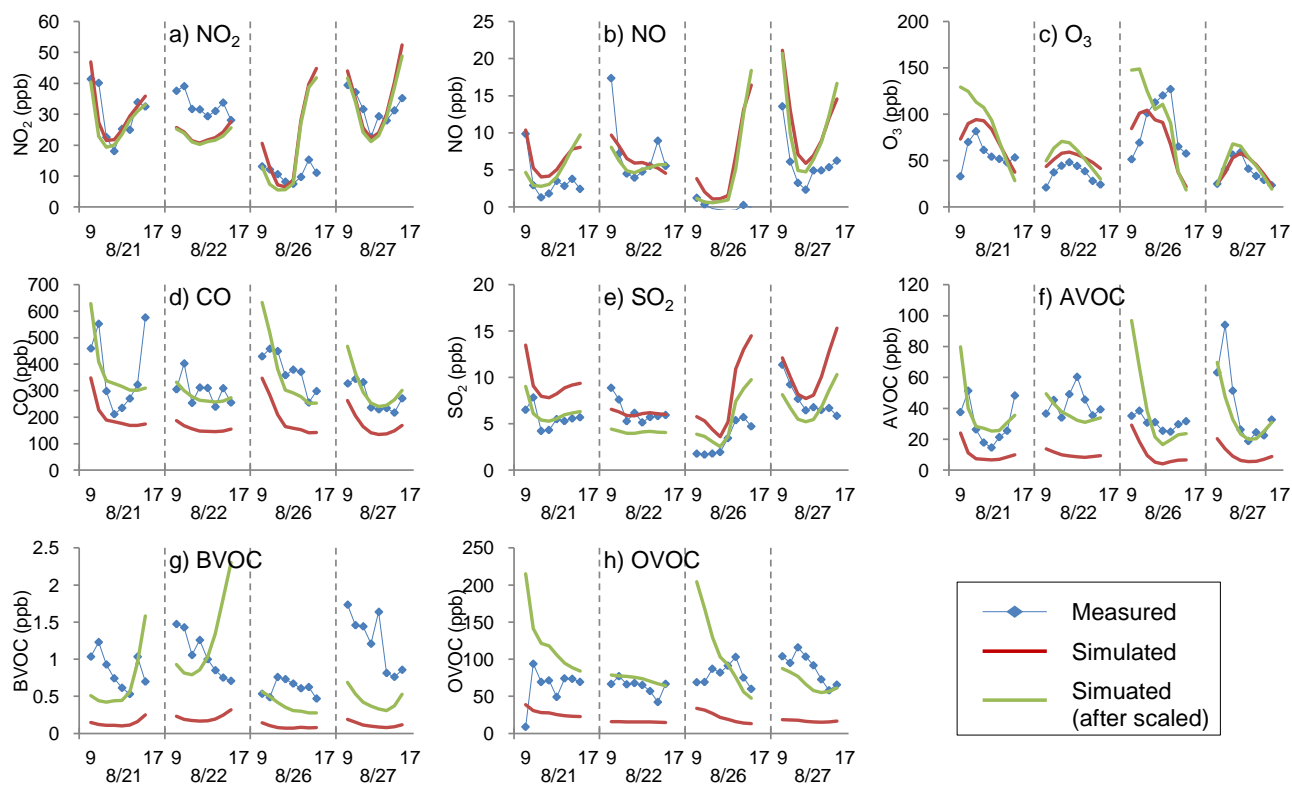


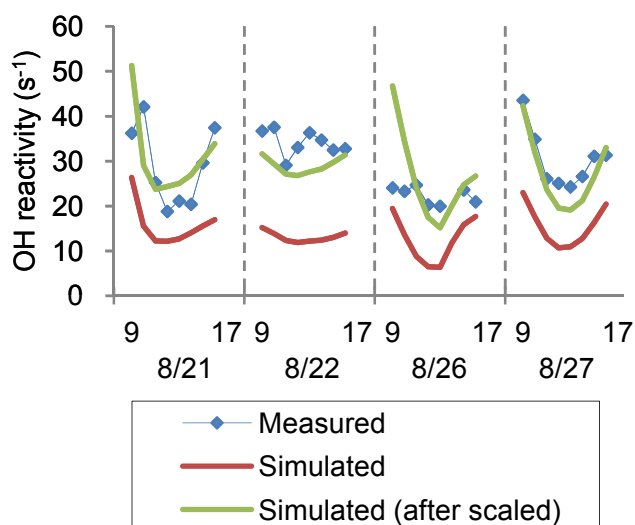
**Fig. 5.** Time series of measured and simulated concentrations of species groups before and after application of scaling factors.

twice to bring the simulated concentrations closer to the measured concentrations. TRP1 is excluded from this procedure, because it is originated from biogenic sources, and uniform scaling factors defined in the metropolitan area may cause a significant overestimation in rural areas. Ratios of the simulated concentrations to the measured concentrations obtained by application of scaling factors are also shown in Fig. 4. Ratios of  $O_3$  and HCHO are not close to 1.0 because they are largely affected by secondary products. Ratio of NO is also high after application of scaling factors. It is sensitive to various external factors because NO concentration and its fraction in  $NO_x$  are low throughout the target period. Relatively small scaling factors determined by  $NO_x$  are not enough to match NO concentration. In addition, NO is largely affected by  $O_3$  in the  $NO+O_3$  reaction. There are difficulties in achieving an agreement between measured and calculated concentrations for these species. Except for these species, the procedure makes the ratios closer to 1.0.

Figure 5 shows time series of the measured and simulated hourly concentrations of species groups before and after application of scaling factors. The absolute level and hourly variations of concentrations of critical species are reproduced well. However, the simulated concentrations of AVOC, BVOC and OVOC are significantly underestimated before application of scaling factors. Application of scaling factors makes their concentrations closer to the measured

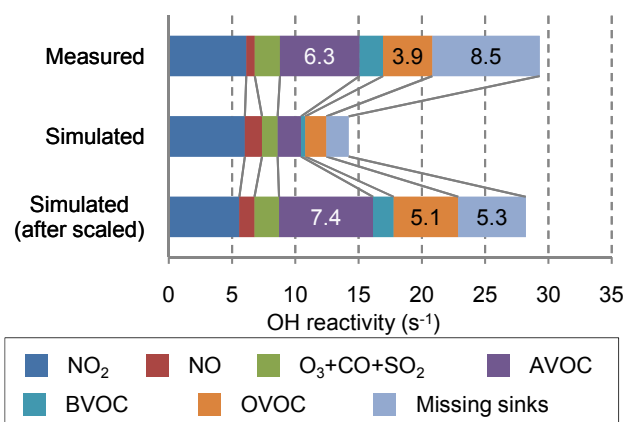
values. Hourly variations of AVOC and OVOC are also reproduced well. Figure 6 shows time series of the measured and simulated hourly total OH reactivity before and after application of scaling factors. Simulated total OH reactivity is calculated from the simulated concentrations of SAPRC99 species and their reaction rate coefficients with OH defined in SAPRC99. The measured total OH reactivity tends to be high in the morning and evening, while low around noon. Such hourly variations in total OH reactivity are reproduced in the simulations; however, the values are underestimated before application of scaling factors. Application of scaling factors also makes the simulated OH reactivity closer to the measured value.

Figure 7 shows the measured and simulated OH reactivity of species groups which is averaged over the target period before and after application of scaling factors. Simulated OH reactivity of critical species shows a good agreement with the measurements. However, the simulated OH reactivity of AVOC, BVOC and OVOC is significantly underestimated before application of scaling factors. The underestimation of these species groups is considered as a major cause of underestimated total OH reactivity. Application of scaling factors makes the simulated total OH reactivity closer to the measured value. However, further considerations are required on the contribution of the species groups to total OH reactivity.



**Fig. 6.** Time series of measured and simulated total OH reactivity before and after application of scaling factors.

As shown in Fig. 4, the simulated concentrations of each species included in AVOC show a good agreement with the measured values, which leads to an expectation that the simulated OH reactivity of AVOC will achieve a good agreement with the measured values. However, the fact is that the simulated OH reactivity of AVOC is higher than the measured value. It indicates that reaction rate coefficients of AVOC with OH in SAPRC99 are higher than those of measured AVOC species. One possible reason is that SAPRC99 assumes the existence of species which are never measured in the observation campaign and having higher reaction rate coefficients with OH than those of measured AVOC species. If such species really exist in the atmosphere, they may be included in the missing sinks in measured total OH reactivity. In addition, not only the simulated OH reactivity but also simulated concentrations of AVOC should be higher than the measured values. Impacts of the missing sinks for which AVOC might account will be discussed in the next section. Another possible reason is that SAPRC99 is not suitable for simulating the atmosphere over Tokyo metropolitan area. A lumping approach in which VOC species are combined into groups is used in SAPRC99, which might result in the differences in measured and calculated OH reactivity of VOC groups over Tokyo metropolitan area. The simulated OH reactivity of OVOC is higher than the measured OH reactivity, simply because HCHO is still overestimated after application of scaling factors. Better agreement may be achieved between measured and simulated OH reactivity if simulated concentrations of HCHO could be agreed with the measured values. The simulated OH reactivity of missing sinks ( $5.3 \text{ s}^{-1}$ ) is lower than the measured value ( $8.5 \text{ s}^{-1}$ ). The simulation can explain about 60% of the measured OH reactivity of missing sinks by species groups



**Fig. 7.** Measured and simulated OH reactivity of species groups which is averaged over the target period before and after application of scaling factors. Contribution of species groups except for missing sinks in measured OH reactivity is obtained from measured concentrations of species and their reaction rate coefficients. OH reactivity of missing sinks in measured OH reactivity is obtained by subtracting sum of OH reactivity of species groups from directly measured OH reactivity.

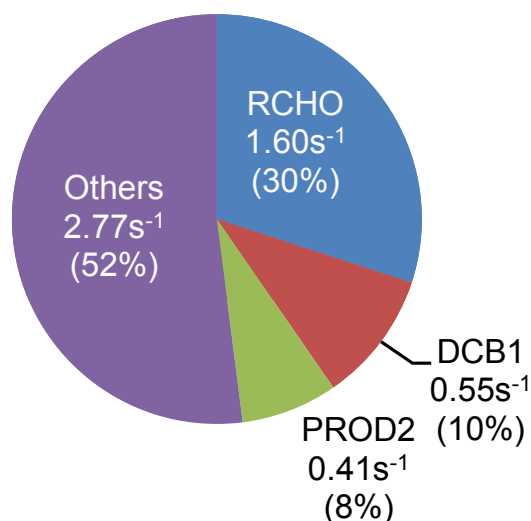
treated in SAPRC99, however, remaining 40% cannot be explained. Impacts of remaining unexplained missing sinks (about  $3.0 \text{ s}^{-1}$ ) will be discussed through sensitivity analyses in the next section.

## 5 Sensitivity analyses of OH missing sinks

As shown in the previous section, the simulated OH reactivity of missing sinks is about  $3.0 \text{ s}^{-1}$  lower than the measured value. Possible candidates for unexplained missing sinks are unknown secondary products and unidentified primary emitted species. Sensitivity analyses are conducted to investigate their impacts on photochemical reactions and secondary product formation in the atmosphere. The simulation in which scaling factors are applied to input emissions and boundary concentrations (described in the previous section) is used as the base case in the sensitivity analyses.

### 5.1 Impacts of unknown secondary products

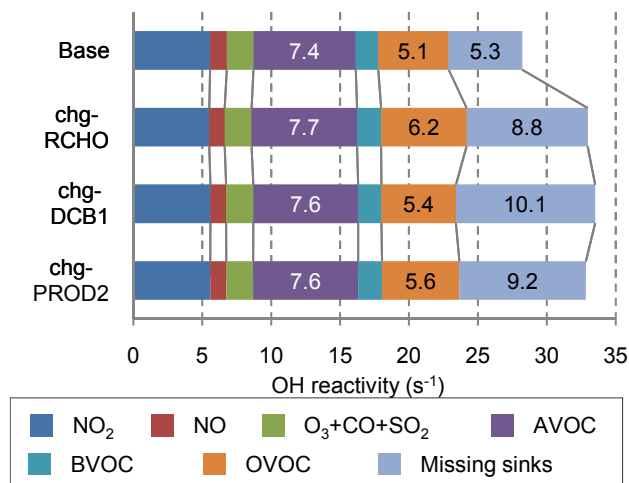
It is impossible to estimate impacts of unknown secondary products because their reaction path and rate coefficients are also unknown. Therefore, we assumed that unknown secondary products have similar characteristics to the known secondary products. Figure 8 shows contribution of SAPRC99 species to the simulated OH reactivity of missing sinks which is averaged over the target period in the base case. RCHO represents a group of aldehydes with three or more carbons, DCB1 represents a group of reactive aromatic fragmentation products that do not undergo significant photodecomposition to radicals,



**Fig. 8.** Contribution of SAPRC species to simulated OH reactivity of missing sinks which is averaged over the target period in the base case.

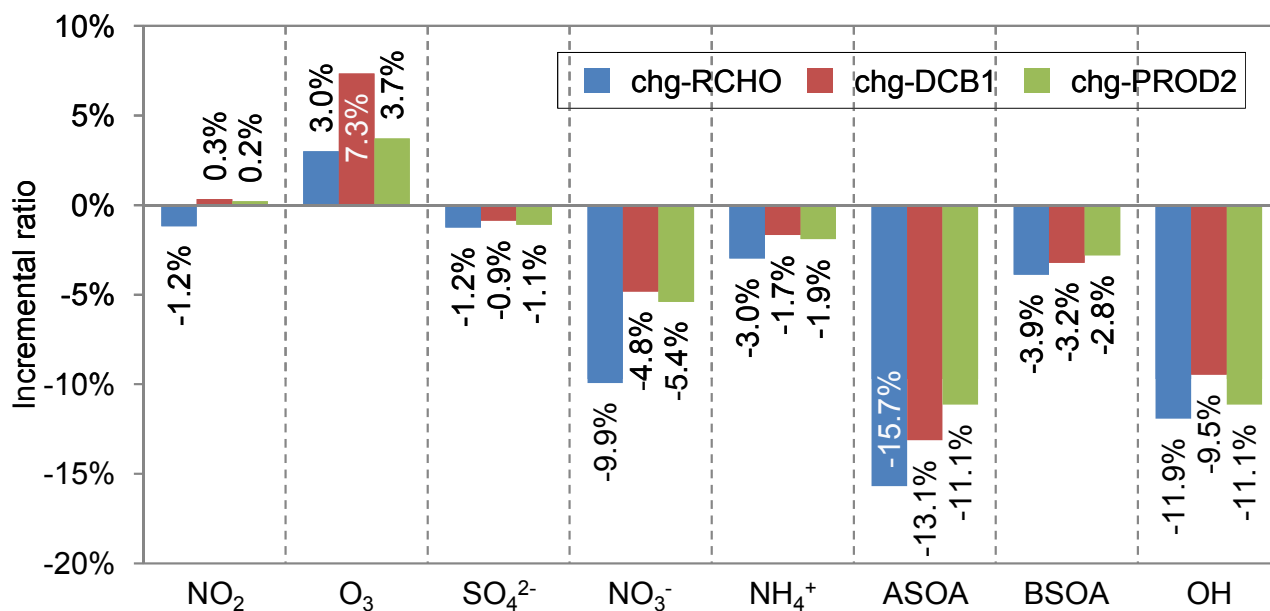
and PROD2 represents a group of ketones and other non-aldehyde oxygenated products which react with OH radicals faster than  $5 \times 10^{-12} \text{ cm}^3 \text{ molec}^{-2} \text{ s}^{-1}$  (Carter, 2000). Contribution of these groups to the simulated OH reactivity of missing sinks is 30% for RCHO, 10% for DCB1 and 8% for PROD2, respectively. They are major secondary products in the simulation, so that their impacts are investigated here. In order to increase their concentrations in sensitivity analyses, factors are multiplied to the individual yield of the groups (RCHO, DCB1 and PROD2) in SAPRC99 reactions, and then simulations are conducted for the three cases: chg-RCHO, chg-DCB1 and chg-PROD2. Multiplied factors to the yields for RCHO, DCB1 and PROD2 to add  $3.0 \text{ s}^{-1}$  to their OH reactivity are 4.6/1.6, 3.6/0.6 and 3.4/0.4, respectively.

Figure 9 shows the simulated OH reactivity of the species groups which is averaged over the target period for the base, chg-RCHO, chg-DCB1 and chg-PROD2 cases. The OH reactivity increases by more than  $3.0 \text{ s}^{-1}$  because increased RCHO, DCB1 and PROD2 form species which react with OH in subsequent reactions. Figure 10 shows incremental ratios of concentrations of  $\text{NO}_2$ ,  $\text{O}_3$ , ambient OH and secondary aerosol components including  $\text{SO}_4^{2-}$ ,  $\text{NO}_3^-$ ,  $\text{NH}_4^+$ , anthropogenic secondary organic aerosol (ASOA) and biogenic SOA (BSOA) in the chg-RCHO, chg-DCB1 and chg-PROD2 cases compared to those in the base case which are averaged over the target period. Those of other remaining species are shown in Fig. S1 in Supplementary material: <http://www.atmos-chem-phys.net/9/8975/2009/acp-9-8975-2009-supplement.pdf>.  $\text{O}_3$  increases slightly while incremental ratios differ among the three cases. The ambient OH decreases in all cases because



**Fig. 9.** Simulated OH reactivity of species groups which is averaged over the target period in the base, chg-RCHO, chg-DCB1 and chg-PROD2 cases.

additional OH is consumed by the increased RCHO, DCB1 and PROD2. As a result, oxidation of the precursors by OH is suppressed, and the decrease is observed in  $\text{SO}_4^{2-}$ ,  $\text{NO}_3^-$ , ASOA and BSOA which are major oxidized products. In addition to oxidation by OH,  $\text{SO}_4^{2-}$  is produced via the aqueous reaction of  $\text{SO}_2$  and  $\text{H}_2\text{O}_2$ ,  $\text{NO}_3^-$  is produced via oxidation of  $\text{NO}_2$  to  $\text{NO}_3$  and  $\text{N}_2\text{O}_5$  by  $\text{O}_3$  and the subsequent heterogeneous reaction with  $\text{H}_2\text{O}$ , and ASOA and BSOA are produced via oxidation of precursors by  $\text{O}_3$  and  $\text{NO}_3$ .  $\text{H}_2\text{O}_2$  and  $\text{NO}_3$  as well as  $\text{O}_3$  increase in all cases, but  $\text{SO}_4^{2-}$ ,  $\text{NO}_3^-$ , ASOA and BSOA decrease. Therefore, oxidation by OH is more influential than reactions with other species in the three cases.  $\text{NH}_4^+$  also decreases because of decreased  $\text{SO}_4^{2-}$  and  $\text{NO}_3^-$ , which are anions coupling mainly with  $\text{NH}_4^+$ .  $\text{NO}_2$  is mainly produced in the  $\text{NO}+\text{O}_3$  reaction, and is oxidized by OH. Production is enhanced by increased  $\text{O}_3$  and oxidation is suppressed by decreased OH. But in fact,  $\text{NO}_2$  decreases in the chg-RCHO case and increase only slightly in the chg-DCB1 and chg-PROD2 cases. Peroxy acyl radicals are major products in the RCHO+OH reaction, and they are converted to peroxy acyl nitrates via the reaction with  $\text{NO}_2$ . Their production appears to compensate increase of  $\text{NO}_2$  especially in the chg-RCHO case. Based on the results described above, missing sinks are considered to suppress formation of secondary aerosol components and enhance formation of ozone in the cases that unknown secondary components may account for the missing sinks which have similar characteristics to RCHO, DCB1 and PROD2.



**Fig. 10.** Incremental ratios of concentrations of NO<sub>2</sub>, O<sub>3</sub>, OH and secondary aerosol components in the chg-RCHO, chg-DCB1 and chg-PROD2 cases compared to those in the base case, which are averaged over the target period.

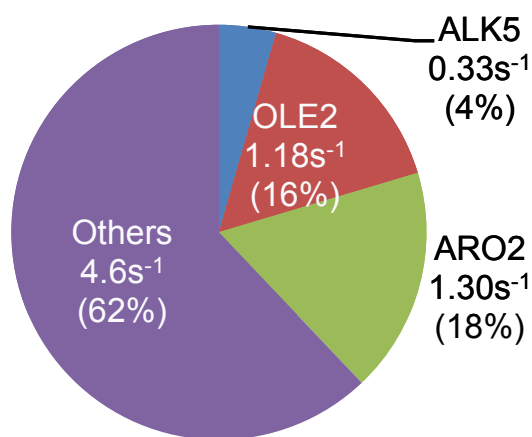


**Fig. 11.** Contribution of SAPRC species to the simulated OH reactivity of AVOC which is averaged over the target period in the base case.

## 5.2 Impacts of unidentified primary emitted species

Figure 11 shows contribution of SAPRC99 species to the simulated OH reactivity of AVOC which is averaged over the target period in the base case. Contribution of ALK5, OLE2 and ARO2 to the simulated OH reactivity of AVOC is 4%, 16% and 18%, respectively. They are aggregated species groups which have the highest reaction rate coefficients with OH among alkanes, olefins and aromatic compounds in SAPRC99. In the previous section, reaction rate coefficients

of SAPRC99 AVOC species are higher than those of measured values. If missing sinks which correspond to AVOC exist in the atmosphere, they are likely to have higher reaction rate coefficients and account for ALK5, OLE2 and ARO2. Therefore, factors are multiplied to input emissions and boundary concentrations of ALK5, OLE2 and ARO2 individually, and then the simulation is conducted for these three cases: chg-ALK5, chg-OLE2 and chg-ARO2. Multiplied factors of ALK5, OLE2 and ARO2 to add 3.0 s<sup>-1</sup> to their OH reactivity are 3.3/0.3, 4.2/1.2 and 4.3/1.3, respectively.

Figure 12 shows the simulated total OH reactivity of the species groups which is averaged over the target period in the base, chg-ALK5, chg-OLE2 and chg-ARO2 cases. The OH reactivity of AVOC increased by about 3.0 s<sup>-1</sup> in the chg-OLE2 and chg-ARO2 cases, while by more than 3.0 s<sup>-1</sup> in the chg-ALK5 case. The OH reactivity of OVOC and missing sinks slightly increases in all cases due to formation of secondary products from increased AVOC, and a resulting increase in the total OH reactivity is more than 3.0 s<sup>-1</sup>. Figure 13 shows incremental ratios of concentrations of NO<sub>2</sub>, O<sub>3</sub> and secondary aerosol components in the chg-ALK5, chg-OLE2 and chg-ARO2 cases compared to those in the base case which is averaged over the target period. Those of other remaining species are shown in Fig. S2 in Supplementary material: <http://www.atmos-chem-phys.net/9/8975/2009/acp-9-8975-2009-supplement.pdf>. Signs and magnitudes of incremental ratios have a wider variety than cases for unknown secondary products. O<sub>3</sub> increases slightly, however, the ratios vary among the three cases. The ambient

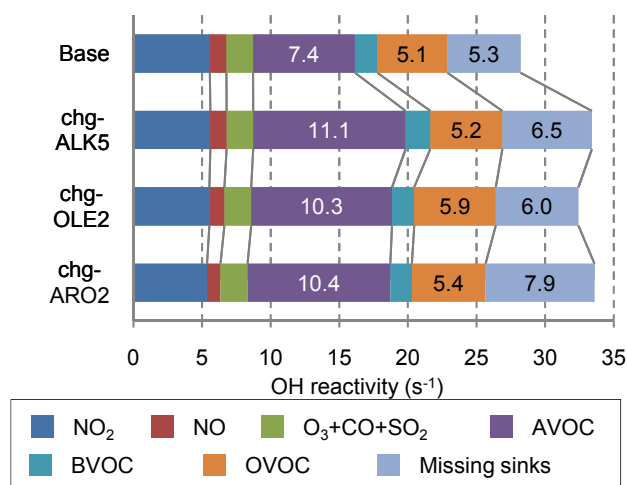


**Fig. 12.** Simulated OH reactivity of species groups which is averaged over the target period in the base, chg-ALK5, chg-OLE2 and chg-ARO2 cases.

OH decreases in the chg-ALK5 case due to increased ALK5. As a result, available ambient OH for the reaction with ALK5 decreases, and then the OH reactivity of AVOC increases by more than  $3.0 \text{ s}^{-1}$  in the chg-ALK5 case. On the other hand, ambient OH slightly increases in the chg-OLE2 and chg-ARO2 cases. It is difficult to identify reasons for increase of ambient OH because concentrations of a lot of species change especially in the chg-ARO2 case as shown in Fig. S2: <http://www.atmos-chem-phys.net/9/8975/2009/acp-9-8975-2009-supplement.pdf>. Products from photochemical reactions of OLE2 and ARO2 seem to contribute to the increase in ambient OH. Changes of  $\text{SO}_4^{2-}$  can be explained clearly by changes of OH and  $\text{H}_2\text{O}_2$ . The situation is much complicated for  $\text{NO}_2$  and  $\text{NO}_3^-$ . In the chg-ALK5 case, production of  $\text{NO}_2$  via the  $\text{NO}+\text{O}_3$  reaction is enhanced by increased  $\text{O}_3$ , and conversion of  $\text{NO}_2$  to  $\text{NO}_3^-$  is suppressed by decreased OH. Therefore,  $\text{NO}_2$  increases but production of organic nitrates diminishes increase of  $\text{NO}_2$ . On the other hand, in the chg-OLE2 and chg-ARO2 cases, conversion of  $\text{NO}_2$  to  $\text{NO}_3^-$  is enhanced by increased OH. However,  $\text{NO}_3^-$  decreases in the chg-OLE2 case because influence of production of peroxy acyl nitrates is larger than conversion to  $\text{NO}_3^-$ . ASOA concentrations increase significantly in the chg-ALK5 and chg-ARO2 cases because ALK5 and ARO2 are precursors of ASOA in SAPRC99. SOA formation is enhanced when organics mass concentrations in particle phase are high (Odum et al., 1996; Schell et al., 2001). Therefore, BSOA also increases in both cases. BSOA is also produced via oxidation of precursors by OH and  $\text{O}_3$ .  $\text{O}_3$  increases only slightly and OH decreases in the ALK5 case. As a result, TRP1, which is a precursor of BSOA, increases while BSOA increases significantly. Therefore, increase of ASOA appears to be main reasons for significant increase of BSOA.

Based on the results described above, it can be said that the impacts of missing sinks are diversified in the cases that missing sinks are unidentified primary emitted species. Some species suppress, while others enhance the oxidation by OH. Some species could increase SOA formation. All of unidentified primary emitted species increase  $\text{O}_3$  formation. In general, a lot of three-dimensional air quality simulations are facing problems of significant underestimation of organic aerosols (Volkamer et al., 2006). Presence of unidentified primary emitted species which are neglected in the simulation but play an important role as ASOA precursors in the atmosphere may be one of the reasons for underestimated organic aerosols.

## 6 Summary

The three-dimensional air quality simulations are applied to the observation campaign which has been conducted in the summer of 2007, during which total OH reactivity and concentrations of various species were measured at the heart of Tokyo metropolitan area. The simulated total OH reactivity is significantly underestimated because of the underestimation of the simulated OH reactivity of AVOC, BVOC, OVOC and missing sinks. Emission inventory data is required to be improved. Concentrations of individual VOC species reflect strength of emissions from specific sources. They can be used as fingerprints of sources. As shown in Fig. 4, ratios of simulated to measured concentrations vary among species. Based on discrepancy between simulated to measured concentrations of individual species groups, overestimated or underestimated VOC sources may be able to be identified. Coupled analyses with the receptor modelling are also desirable. However, databases are not enough to conduct such analyses. Data on VOC emission profiles of various sources as well as ambient concentrations of individual VOC species are scarce in Japan. More measurement data at different places and periods are needed to contribute to a thorough improvement of the emission inventory.

After application of scaling factors to input emissions and boundary concentrations, a good agreement is obtained between the simulated concentrations of most species groups and the measured concentrations. However, the simulated OH reactivity of missing sinks is still underestimated. This result implies that simulations are not accurate enough in terms of photochemical reactions even if concentrations of major species are simulated well. Based on the results of sensitivity analyses, unidentified missing sinks could suppress formation of secondary aerosol components and enhance formation of  $\text{O}_3$ , while could increase SOA production significantly if SOA precursors account for the missing sinks.

The range of incremental ratios of concentrations in sensitivity analyses can be regarded as one of potential uncertainties in the three-dimensional air quality simulations in terms of photochemical reactions. Identifying the missing sinks

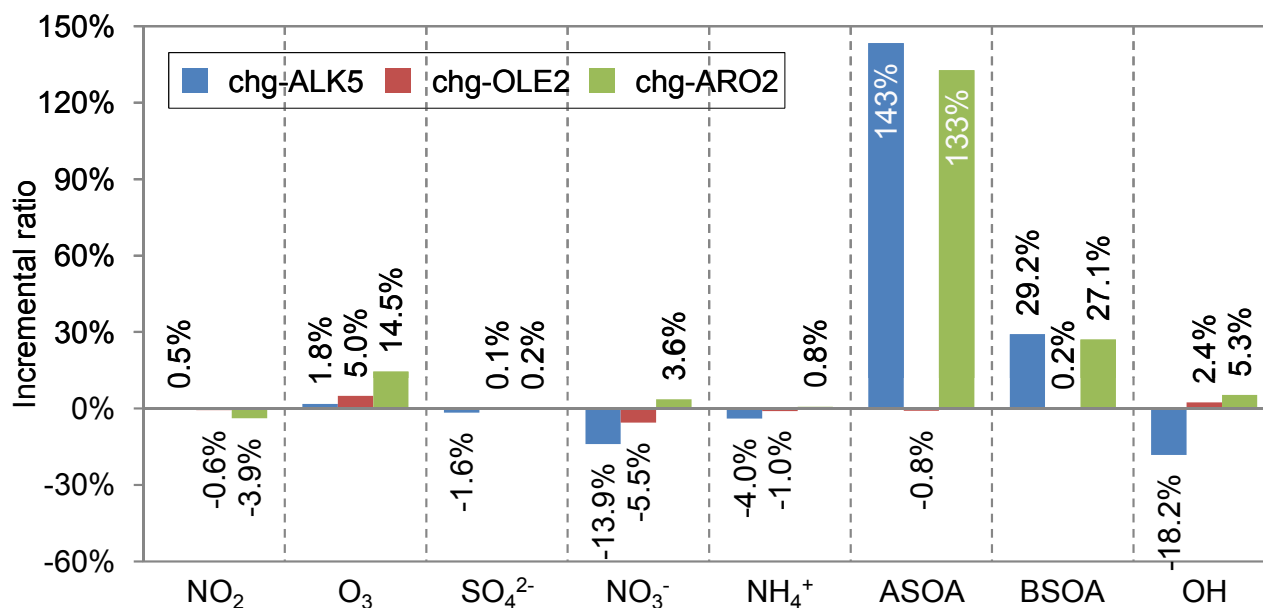


**Fig. 13.** Incremental ratios of concentrations of NO<sub>2</sub>, O<sub>3</sub>, OH and secondary aerosol components in the chg-ALK5, chg-OLE2 and chg-ARO2 cases compared to those in the base case, which are averaged over the target period.

and revealing their photochemical reaction path and rate coefficients are essential to reduce the uncertainties. Advances in measurement instruments and techniques will be required to identify the missing sinks.

*Acknowledgements.* This study was conducted as part of Japan Auto-Oil Program (JATOP) which is a joint research program between automobile and petroleum industries and administered by Japan Petroleum Energy Center.

Edited by: A. Hofzumahaus

## References

- Atkinson, R.: Gas-phase tropospheric chemistry of organic compounds, *J. Phys. Chem. Ref. Data, Monograph*, 2, 1–216, 1994.
- Atkinson, R.: Gas-phase tropospheric chemistry of volatile organic compounds, 1. Alkanes and alkenes, *J. Phys. Chem. Ref. Data*, 26, 215–290, 1997.
- Atkinson, R., Baulch, D. L., Cox, R. A., Hampson, R. F., Kerr, J. A., Rossi, M. J., and Troe, J.: Evaluated kinetic and photochemical data for atmospheric chemistry: Supplement VI – IUPAC subcommittee on gas kinetic data evaluation for atmospheric chemistry, *J. Phys. Chem. Ref. Data*, 26, 1329–1499, 1997.
- Byun, D. and Schere, K. L.: Review of the governing equations, computational algorithms, and other components of the Models-3 Community Multiscale Air Quality (CMAQ) modeling system, *Appl. Mech. Rev.*, 59, 51–77, 2006.
- Calvert, J. G., Derwent, R. G., Orlando, J. J., Tyndall, G. S., and Wallington, T. J.: *Mechanisms of Atmospheric Oxidation of the Alkanes*, Oxford University Press, New York, 1008 pp., 2008.
- Carter, W. P. L.: Implementation of the SAPRC-99 chemical mechanism into the models-3 framework, Report to the United States Environmental Protection Agency, 2000.
- Di Carlo, P., Brune, W. H., Martinez, M., Harder, H., Leshner, R., Ren, X., Thornberry, T., Carroll, M. A., Young, V., Shepson, P. B., Riemer, D., Apel, E., and Campbell, C.: Missing OH reactivity in a forest: Evidence for unknown reactive biogenic VOCs, *Science*, 304, 722–725, 2004.
- Gery, M. W., Whitten, G. Z., Killus, J. P., and Dodge, M. C.: A photochemical kinetics mechanism for urban and regional scale computer modelling, *J. Geophys. Res.*, 94, 12925–12956, 1989.
- Guenther, A., Karl, T., Harley, P., Wiedinmyer, C., Palmer, P. I., and Geron, C.: Estimates of global terrestrial isoprene emissions using MEGAN (Model of Emissions of Gases and Aerosols from Nature), *Atmos. Chem. Phys.*, 6, 3181–3210, 2006, <http://www.atmos-chem-phys.net/6/3181/2006/>.
- Hofzumahaus, A., Rohrer, F., Lu, K., Bohn, B., Brauers, T., Chang, C.-C., Fuchs, H., Holland, F., Kita, K., Kondo, Y., Li, X., Lou, S., Shao, M., Zeng, L., Wahner, A., and Zhang, Y.: Amplified trace gas removal in the troposphere, *Science*, 324, 1702–1704, 2009.
- Japan Petroleum Energy Center: [http://www.pecj.or.jp/english/jcap/jatop/index\\_jatop.html](http://www.pecj.or.jp/english/jcap/jatop/index_jatop.html), last access: 7 July 2009, 2009.
- Kannari, A., Tonooka, Y., Baba, T., and Murano, K.: Development of multiple-species 1 km × 1 km resolution hourly basis emissions inventory for Japan, *Atmos. Environ.*, 41, 3428–3439, 2007.
- Meng, Z., Dabdub, D., and Seinfeld, J. H.: Chemical coupling between atmospheric ozone and particulate matter, *Science*, 277, 116–119, 1997.
- Ministry of the Environment: <http://www.env.go.jp/air/osen/index.html>, last access: 7 July 2009, 2008.
- Mao, J., Ren, X., Brune, W. H., Olson, J. R., Crawford, J. H., Fried, A., Huey, L. G., Cohen, R. C., Heikes, B., Singh, H. B., Blake,

- D. R., Sachse, G. W., Diskin, G. S., Hall, S. R., and Shetter, R. E.: Airborne measurement of OH reactivity during INTEX-B, *Atmos. Chem. Phys.*, 9, 163–173, 2009, <http://www.atmos-chem-phys.net/9/163/2009/>.
- Nakashima, Y., Matsuda, H., Ide, S., Miyazaki, K., Yamazaki, K., Okazaki, H., Osada, T., Tajima, Y., Suthawaree, J., Kato, S., Shimo, N., Matsunaga, S., Apel, E., Greenberg, J., Guenther, A., Ueno, H., Sasaki, H., Hoshi, J., Yoshino, A., Yokota, H., Ishii, K., and Kajii, Y.: Diagnosis of urban air quality by measurement of total OH reactivity II: Comprehensive observations in the urban of Tokyo, *J. Jpn. Soc. Atmos. Environ.*, 44, 33–41, 2009.
- Nansai, K., Suzuki, N., Tanabe, K., Kobayashi, S., and Moriguchi, Y.: Design of Georeference-Based Emission Activity Modeling System (G-BEAMS) for Japanese emission inventory management, in: Proceedings of the 13th International Emission Inventory Conference in Clearwater, Florida, USA, 7–10 June, 2004.
- Odum, J. R., Hoffmann, T., Bowman, F., Collins, D., Flagan, R. C., and Seinfeld, J. H.: Gas/particle partitioning and secondary organic aerosol yields, *Environ. Sci. Technol.*, 30, 2580–2585, 1996.
- Ohara, T., Akimoto, H., Kurokawa, J., Horii, N., Yamaji, K., Yan, X., and Hayasaka, T.: An Asian emission inventory of anthropogenic emission sources for the period 1980–2020, *Atmos. Chem. Phys.*, 7, 4419–4444, 2007, <http://www.atmos-chem-phys.net/7/4419/2007/>.
- Ren, X. R., Harder, H., Martinez, M., Leshner, R. L., Olinger, A., Shirley, T., Adams, J., Simpas, J. B., and Brune, W. H.: HO<sub>x</sub> concentrations and OH reactivity observations in New York City during PMTACS-NY2001, *Atmos. Environ.*, 37, 3627–3637, 2003.
- Sadanaga, Y., Yoshino, A., Kato, S., Yoshioka, A., Watanabe, K., Miyakawa, Y., Hayashi, I., Ichikawa, M., Matsumoto, J., Nishiyama, A., Akiyama, N., Kanaya, Y., and Kajii, Y.: The importance of NO<sub>2</sub> and volatile organic compounds in the urban air from the viewpoint of the OH reactivity, *Geophys. Res. Lett.*, 31, L08102, doi:10.1029/2004GL019661, 2004a.
- Sadanaga, Y., Yoshino, A., Watanabe, K., Yoshioka, A., Wakazono, Y., Kanaya, Y., and Kajii, Y.: Development of a measurement system of OH reactivity in the atmosphere by using a laser-induced pump and probe technique, *Rev. Sci. Instrum.*, 75, 2648–2655, 2004b.
- Sadanaga, Y., Kondo, S., Hashimoto, K., and Kajii, Y.: Measurement of the rate coefficient for the OH+NO<sub>2</sub> reaction under the atmospheric pressure: Its humidity dependence, *Chem. Phys. Lett.*, 419, 474–478, 2005a.
- Sadanaga, Y., Yoshino, A., Kato, S., and Kajii, Y.: Measurements of OH reactivity and photochemical ozone production in the urban atmosphere, *Environ. Sci. Technol.*, 39, 8847–8852, 2005b.
- Sander, S. P., Friedl, R. R., Golden, D. M., Kurylo, M. J., Huie, R. E., Orkin, V. L., Moortgat, G. K., Ravishankara, A. R., Kolb, C. E., Molina, M. J., and Finlayson-Pitts, B. J.: Chemical kinetics and photochemical data for use in atmospheric studies, Evaluation No. 14, JPL Publication 02–25, 2003.
- Schell, B., Ackermann, I. J., Hass, H., Binkowski, F. S., and Ebel, A.: Modeling the formation of secondary organic aerosol within a comprehensive air quality model system, *J. Geophys. Res.*, 106, 28275–28293, 2001.
- Shirley, T. R., Brune, W. H., Ren, X., Mao, J., Leshner, R., Cardenas, B., Volkamer, R., Molina, L. T., Molina, M. J., Lamb, B., Velasco, E., Jobson, T., and Alexander, M.: Atmospheric oxidation in the Mexico City Metropolitan Area (MCMA) during April 2003, *Atmos. Chem. Phys.*, 6, 2753–2765, 2006, <http://www.atmos-chem-phys.net/6/2753/2006/>.
- Sinha, V., Williams, J., Crowley, J. N., and Lelieveld, J.: The Comparative Reactivity Method - a new tool to measure total OH Reactivity in ambient air, *Atmos. Chem. Phys.*, 8, 2213–2227, 2008, <http://www.atmos-chem-phys.net/8/2213/2008/>.
- Skamarock, W. C., Klemp, J. B., Dudhia, J., Gill, D. O., Barker, D. M., Wang, W., and Powers, J. G.: A description of the advanced research WRF version 2, NCAR Technical Note, NCAR/TN-468+STR, 2005.
- Steiner, A. L., Cohen, R. C., Harley, R. A., Tonse, S., Millet, D. B., Schade, G. W., and Goldstein, A. H.: VOC reactivity in central California: comparing an air quality model to ground-based measurements, *Atmos. Chem. Phys.*, 8, 351–368, 2008, <http://www.atmos-chem-phys.net/8/351/2008/>.
- Stroud, C. A., Morneau, G., Makar, P. A., Moran, M. D., Gong, W., Pabla, B., Zhang, J., Bouchet, V. S., Fox, D., Venkatesh, S., Wang, D., and Dann, T.: OH-reactivity of volatile organic compounds at urban and rural sites across Canada: Evaluation of air quality model predictions using speciated VOC measurements, *Atmos. Environ.*, 42, 7746–7756, 2008.
- Volkamer, R., Jimenez, J. L., San Martini, F., Dzepina, K., Zhang, Q., Salcedo, D., Molina, L. T., Worsnop, D. R., and Molina, M. J.: Secondary organic aerosol formation from anthropogenic air pollution: Rapid and higher than expected, *Geophys. Res. Lett.*, 33, L17811, doi:10.1029/2006GL026899, 2006.
- Yoshikado, H.: Numerical study of the daytime urban effect and its interaction with the sea breeze, *J. Appl. Meteorol.*, 31, 1146–1164, 1992.
- Yoshino, A., Sadanaga, Y., Watanabe, K., Kato, S., Miyakawa, Y., Matsumoto, J., and Kajii, K.: Measurement of total OH reactivity by laser-induced pump and probe technique - comprehensive observations in the urban atmosphere of Tokyo, *Atmos. Environ.*, 40, 7869–7881, 2006.